CARM1 (PRMT4) acts as a transcriptional coactivator during retinoic acid-induced embryonic stem cell differentiation

Cynthia M. Quintero[1, 2, 4], Kristian B. Laursen[1], Nigel P. Mongan[1, 3], Minkui Luo[2], and Lorraine J. Gudas[1*]

1. Department of Pharmacology, Weill Cornell Medical College of Cornell University, New York, NY, USA.
2. Molecular Pharmacology and Chemistry Program, Memorial Sloan-Kettering Cancer Center, New York, NY, USA.
3. Faculty of Medicine and Health Sciences, School of Veterinary Medicine and Science, The University of Nottingham, Sutton Bonington Campus, Loughborough, UK.
4. Weill Cornell Graduate School of Medical Sciences – Pharmacology Program, Weill Cornell Medical College of Cornell University, New York, NY, USA.

*To whom correspondence should be addressed: Dr. Lorraine J. Gudas, Department of Pharmacology, Weill Cornell Medical College, 1300 York Avenue, New York, NY 10065, USA. Tel: (212) 746-6250; Fax: (212) 746-8858; Email: ljgudas@med.cornell.edu

Key words: CARM1, retinoic acid, NR2F1/Coup-TF1, CRABP2, epigenetic marks

ABSTRACT

Activation of the retinoic acid (RA) signaling pathway is important for controlling embryonic stem cell differentiation and development. Modulation of this pathway occurs through the recruitment of different epigenetic regulators at the retinoic acid receptors (RARs) located at retinoic acid responsive elements (RAREs) and/or RA-responsive regions of RA-regulated genes. Coactivator-associated arginine methyltransferase 1 (CARM1, PRMT4) is a protein arginine methyltransferase that also functions as a transcriptional coactivator. Previous studies highlight CARM1's importance in the differentiation of different cell types. We address CARM1 function during RA-induced differentiation of murine embryonic stem cells (mESCs) using shRNA lentiviral transduction and CRISPR/Cas9 technology to deplete CARM1 in mESCs. We identify CARM1 as a novel transcriptional coactivator required for the RA-associated decrease in Rex1 (Zfp42), and for the RA induction of a subset of RA-regulated genes, including *CRABP2* and *NR2F1* (*Coup-TF1*). Furthermore, CARM1 is required for mESCs to differentiate into extraembryonic endoderm in response to RA. We next characterize the epigenetic mechanisms that contribute to RA-induced transcriptional activation of *CRABP2* and *NR2F1* in mESCs and show for the first time that CARM1 is required for this activation. Collectively, our data demonstrate that CARM1 is required for transcriptional activation of a subset of RA target genes, and we uncover changes in the recruitment of Suz12 and the epigenetic H3K27me3 and H3K27ac marks at gene regulatory regions for *CRABP2* and *NR2F1* during RA-induced differentiation.

INTRODUCTION

        The processes by which stem cells are able to maintain their self-renewal

potential versus undergo differentiation are of intense interest given the potential

therapeutic applicability of stem cell manipulation. Embryonic stem cells (ESCs)

undergo differentiation in the presence of the vitamin A metabolite, retinoic acid (RA),

via activation of nuclear retinoic acid receptors (RAR α, β, & γ), members of the nuclear

receptor (NR) family of proteins[1, 2]. The retinoid X receptor (RXR)/RAR heterodimer is

bound to DNA at retinoic acid responsive elements (RAREs) of specific RA-regulated

genes[1]. The ability of stem cells to differentiate along several cell lineages is in part a

result of the regulation by RA signaling of post-translational modifications (PTMs) of

proteins, including chromatin, by various epigenetic regulators[2]. Specifically, binding of

the agonist RA to the RARs results in rapid loss of the epigenetic regulatory polycomb

repressive complex 2 (PRC2) from various RAREs and promoter regions of RA

responsive genes; this is accompanied by the transcriptional activation of these genes

involved in cell differentiation[1-3]. These RA-associated changes in covalent

modifications occur on both histone and non-histone proteins[1, 3].

        Lysine methylation is one modification that is associated with transcriptional

activation or repression of genes during ESC differentiation by RA, depending on the

specific lysine modified[1]. This network of epigenetic regulation has been widely studied

in the model system of RA-induced ESC differentiation[1]. Another important, but less

well understood modification in the context of RA-induced ESC differentiation is arginine

methylation by protein arginine methyltransferases (PRMTs)[4, 5], the focus of this work.

        Protein arginine methylation plays a role in various cellular processes, such as

transcriptional control and cell signaling[6-11]. PRMTs methylate their substrates via the

enzymatic transfer of a methyl group from the S-adenosyl-L-methionine cofactor (SAM) to the guanidino nitrogens of arginine residues[12, 13]. PRMT1, PRMT6, and PRMT8 play roles in RA-induced neuronal differentiation of ESCs[4, 5]. PRMT1 and PRMT6 both limit the transcriptional activation of some RA-inducible target genes[4, 5], while PRMT8 is required for the activation of specific neuronal genes[4]. Coactivator-associated arginine methyltransferase 1 (CARM1, also referred to as PRMT4) functions as a coactivator of several NR family proteins, including estrogen receptor alpha (ERα) and the androgen receptor (AR)[11, 14-16]. CARM1 mediates transcriptional activation of NR downstream targets via association with other coactivators, such as p300/CBP[10, 17]. Direct methylation of p300/CBP by CARM1 alters p300/CBP function[10]. However, though there is evidence that CARM1 indirectly interacts with RARs in an RXR/RAR chromatin-based *in vitro* transcription system to mediate transcriptional activation[10], the effects of CARM1 on RA target genes have not been characterized in ESCs. Here we delineate the role of CARM1 in ESC RA-induced differentiation.

RESULTS

Generation and characterization of stable mCARM1 shRNA knockdown (KD) and CRISPR/Cas9 knockout (KO) murine embryonic stem cell (mESC) lines.

We first demonstrated that CARM1 is expressed during mESC RA-induced differentiation (Fig. 1A-B). We next analyzed the functions of CARM1 during this differentiation. To assess the role of CARM1 in ESCs we used shRNA lentiviral transduction[18] to generate a stable knockdown (KD) of CARM1 in J1 parental (WT) mESCs (cell line #9117). We confirmed decreased CARM1 transcript and protein levels in the CARM1 KD line in comparison to the J1 WT and shRNA control (shCtl) mESCs (Fig 1C). CARM1 protein levels were 97.3% ± 1.5% SE lower than in WT cells, while CARM1 levels in shCtl and WT cells were similar (98.1% ± 14.2% SE). To confirm decreased CARM1 function, we measured protein levels of me-PABP1 (methylated-Poly(A)-binding protein 1), an established non-histone protein target of CARM1[19]. Levels of me-PABP1 were also 81.1% ± 5.0% SE lower in the CARM1 KD compared to WT (Fig. 1D), indicating that CARM1 activity is also much lower in the CARM1 KD cells. Low, residual levels of CARM1 in an MCF7 CARM1 KD cell line had an impact on the level of its me-PABP1 substrate [20]. Thus, to abolish CARM1 activity completely in mESCs we next generated a CARM1$^{-/-}$ (KO) J1 mESC line using CRISPR-Cas9 technology (cell line #23). CARM1 protein was undetectable in the *CARM1 KO* cell line in comparison to the WT and the shRNA CARM1 KD cell line (Fig. 1C). Similarly, we did not detect any me-PABP1 protein in the *CARM1 KO* (Fig. 1D), indicating that CARM1 activity is lost in the *CARM1 KO* cell line.

CARM1 methylates numerous cellular proteins, and loss of CARM1 function could potentially impair cellular proliferation. We found no changes in cell proliferation in

the stable CARM1 KD and *CARM1 KO* cell lines compared to both WT and the shCtl mESCs (Fig. 1E). This result indicates that CARM1 depletion has no effect on the rate of mESC proliferation.

Stable CARM1 knockout does not affect pluripotency but does prevent the RA-associated decrease in Rex1 (Zfp42).

Previous research has shown that transient CARM1 depletion in human and murine embryonic stem cells (hESC and mESC, respectively) via siRNA methodology results in the initiation of cellular differentiation[21, 22]. To address whether stable lack of CARM1 affects pluripotency, we used qRT-PCR to measure the transcript levels of key pluripotency genes, including *Nanog*, *Oct4*, *Rex1*, and *Sox2*, in our stable CARM1 KD and *CARM1 KO* cell lines in comparison to WT. We found no differences in the levels of these transcripts in the absence of RA in the three cell lines (Fig. 2A). Additionally, we did not detect any differences in Nanog and Oct4 protein levels between the WT and *CARM1 KO* cells (Fig. 2B). Since RA decreases the transcripts of *Nanog*, *Oct4*, *Rex1*, and *Sox2* in differentiating WT mESCs[1, 2], we ascertained if the loss of CARM1 affects these transcript levels. Interestingly, we found that loss of CARM1 prevented the decrease in *Rex1 (Zfp42)* transcripts in response to RA, whereas *Nanog, Oct4* and *Sox2* mRNAs were similar in *CARM1 KO* mESCs compared to RA-treated WT mESCs (Fig. 2A). This implicates CARM1 as a regulator of Rex1, a key pluripotency-associated gene.

Decreased CARM1 level reduces transcript levels of a subset of RA-inducible genes.

We next identified transcripts that changed between the WT and the CARM1 KD cells upon RA addition. Given the role of CARM1 as a histone methyltransferase that

deposits activating epigenetic marks[13] and as a coactivator of other NRs[11, 14-16], we

hypothesized that the lack of CARM1 would limit RA-regulated gene transcription. We

treated J1 WT, shCtl, and CARM1 KD cells with vehicle (0.1% EtOH) or 1 µM RA for 48

hrs and measured the transcript levels of a number of well characterized RA-inducible

genes, including *CRABP2*, *Cyp26b1*, *HoxA1, NR2F1,* and *NR2F2*; these genes play key

roles during RA-induced differentiation of ESCs[1, 2]. For example, CRABP2 and Cyp26b1

are involved in RA metabolism and transport[23-25]. CRABP2 is responsible for

transporting RA from the cytoplasm into the nucleus[25]. Hoxa1 is a transcription factor

required for ESC differentiation into neuronal cells[26] and NR2F1 is involved in RA-

induced parietal endoderm differentiation[27]. We showed that CARM1 depletion

diminished RA-induction of some of the transcripts measured (Fig. 3A-B), suggesting

different classes of RA-inducible genes. We found that *CRABP2*, *Cyp26b1*, *NR2F1,* and

NR2F2 transcripts were induced to a lesser extent in the RA treated CARM1 KD

compared to RA treated WT and shCtl cell lines (Fig. 3A-B). We also found that

CRABP2, *Cyp26b1*, *NR2F1*, and *NR2F2* transcripts were induced to a lesser degree in

the *CARM1 KO* compared to the WT cells (Fig. 3A-B). In contrast, we found that *Hoxa1*

and *RARβ₂* transcripts were induced to similar levels in all four cell lines after RA

addition, indicating that CARM1 depletion had no detectable effect on the RA-induced

increase in *Hoxa1* and *RARβ₂* mRNAs (Fig. 3A-B).

To extend and validate our semi-qPCR results, we treated the J1 WT, shCtl, and

CARM1 KD cell lines with or without 1 µM RA for 48 hrs and performed genome-wide

transcriptomics. By analyzing our RNA-seq data we generated a list of 101 genes

whose RA-induced transcript levels were altered by at least 2-fold in the absence of

CARM1 (Supplemental Table 1). *CRABP2*, *Cyp26b1*, *NR2F1*, and *NR2F2* were present

among these 101 genes, further supporting our initial data focused on genes in the RA

signaling pathway (Fig. 3).

CARM1 depletion decreases RA-induced extraembryonic endoderm gene

expression.

Previously our lab has shown that overexpression of NR2F1 in J1 mESCs

enhances the RA-induction of the extraembryonic endoderm marker genes *Gata4*,

Gata6, *Lamβ1*, and *Sox17*[27]. These genes, and *PDGFRα* and *Sox 7* are definitive

markers of differentiated, extraembryonic endoderm cells[28]. Therefore, we measured

these transcripts at 48 and 72 hrs after RA addition to assess the functional

consequences of the reduced NR2F1 induction observed in the absence of CARM1

(Fig. 4, and by qRT-PCR in Supplemental Fig. 1). Since residual levels of CARM1 can

impact its substrates[20] we only used the *CARM1 KO* in which CARM1 is completely

absent (Fig. 1C). *Gata6* transcripts were induced to a lesser degree in the *CARM1 KO*

than in WT cells by RA by 67.1% ± 4.2% SE (p<0.0001) and 67.5% ± 4.9% SE

(p<0.0001) after 48 and 72 hrs RA addition, respectively (Fig. 4A-B). After 72 hrs of RA

treatment *Gata4*, *Lamβ1*, *PDGFRα*, and *Sox7* transcript levels in the *CARM1 KO* were

73.0% ± 12.5% SE (p<0.0001), 55.6% ± 3.6% SE (p<0.0001), 59.4.0% ± 6.0% SE

(p<0.0001), and 44.5% ± 12.5% SE (p<0.05), respectively, of levels in the J1 WT cells

(Fig. 4A-B). Moreover, Sox17 transcripts were not detectable in the *CARM1 KO*

compared to the J1 WT cells at 72 hrs after RA addition. The minimal induction of

Gata4, *Gata6*, *Lamβ1*, *PDGFRα*, *Sox7*, and *Sox17* transcripts in *CARM1 KO* cells

indicates that CARM1 enhances RA-induced, extraembryonic endoderm differentiation

of mESCs because CARM1 is needed for the increase in *NR2F1* transcripts by RA.

8

CARM1 associates with the RA-inducible target genes with and without RA treatment.

We next investigated the mechanism(s) by which lack of CARM1 affects transcriptional activation during RA-induced ESC differentiation. Since CARM1 acts as a coactivator of other NRs[11, 14, 16], we performed ChIP-qPCR analysis on J1 WT cells treated with or without RA for 24-72 hrs. We focused on identifying CARM1 occupancy near known RARE sites of *CRABP2*, specifically RARE1[24], and the *NR2F1* P_{RefSeq} promoter RA responsive region previously characterized in our lab[18] (Fig. 5A). In parallel, we measured the binding of CARM1 near the known RARE site of *Hoxa1*[29] (Fig. 5A), since RA-induced activation of Hoxa1 is not affected by CARM1 depletion (Fig. 3A-B). We found that CARM1 is present near the *Hoxa1* and *CRABP2* RAREs and near the *NR2F1* P_{RefSeq} promoter in the absence of RA (Fig. 5B). Furthermore, upon addition of RA CARM1 binding did not increase near the RARE1 of *CRABP2* or the P_{RefSeq} region of *NR2F1* (Fig. 5B), suggesting that in J1 WT cells CARM1 association with CRABP2 and NR2F1 is not dynamically regulated in response to RA. Similarly, we detected H3R17me2a near the RARE1 of *CRABP2* and the P_{RefSeq} region of *NR2F1,* and this mark did not increase after RA addition (Supplemental Fig. 2). We note that CARM1 association with CRABP2 and NR2F1 follows the overall levels of CARM1 protein (compare with Fig. 1B).

CARM1 depletion affects the chromatin signatures on a subset of RA-inducible target genes.

Histone tails are subject to multiple covalent modifications, which can function synergistically or antagonistically. These modifications placed by different histone modifying enzymes can occur on neighboring or nearby amino acid residues and adds

another mechanism by which genes are regulated[30]. For example, acetylation of lysine (K) 18 on Histone 3 (H3) by CBP/p300 is required prior to H3R17 dimethylation by CARM1 near the ERα target gene pS2[31]. Given the proximity of K18 and R17, CARM1 depletion may affect the dynamic interaction between these two different epigenetic marks, implicating CARM1 methylation activity in the regulation of RA-inducible genes. CARM1 also mediates dimethylation of R26 on H3[13], which is adjacent to K27 on H3. The trimethylation of H3K27 is often associated with transcriptional repression[32] and the trimethyl mark is deposited by the Suz12 containing-PRC2 complex near the *NR2F1* P_{RefSeq} promoter[18]. For this reason, we measured the effects of the CARM1 knockout on the association of Suz12, a core component of the PRC2 complex, and on the H3K27me3 levels with the P_{RefSeq} region of *NR2F1* and the RARE1 of *CRABP2* after RA addition.

Our results show that Suz12 binding decreases near *NR2F1* P_{RefSeq} in RA treated WT cells, but not in *CARM1 KO* cells. Levels of Suz12 are 1.43-fold ± 0.06 SE ($p<0.01$) and 1.65-fold ± 0.18 SE ($p<0.05$) higher in the KO cells compared to WT at 48 and 72 hrs of RA treatment, respectively (Fig. 6A). In contrast, levels of Suz12 near the *CRABP2* RARE1 did not change with addition of RA to WT cells, but Suz12 levels near the *CRABP2* RARE1 were 2.09-fold ± 0.06 SE ($p<0.01$) and 1.82-fold ± 0.05 SE ($p<0.01$) higher in the KO cells at 48 and 72 hrs of RA treatment, respectively, than in WT cells. Suz12 levels were similar in WT and *CARM1 KO* cells near the *Hoxa1* RARE, with and without RA (Fig. 6A). These data show that the lack of CARM1 increases Suz12 association with RA responsive regions in *NR2F1* and *CRABP2*, but not in *Hoxa1*.

Since PRC2 deposits the repressive H3K27me3 mark, we measured H3K27me3

occupancy near the same genomic regions. We found that while H3K27me3 levels gradually decrease near the *NR2F1* P$_{RefSeq}$ region in WT cells following RA treatment, H3K27me3 levels increase in the *CARM1 KO* cells. Specifically, H3K27me3 levels near *NR2F1* P$_{RefSeq}$ are increased by 2.70-fold ± 0.52 SE (p<0.05) in the *CARM1 KO* cells compared to the WT cells after 72 hrs RA treatment (Fig. 6B). H3K27me3 levels near the *CRABP2* RARE1 do not change with the addition of RA in the WT cells and these levels are similar in the *CARM1 KO* cells (Fig. 6B). When we compare the H3K27me3 marks near the *Hoxa1* RARE we see similar decreases in H3K27me3 levels in WT and *CARM1 KO* cells after RA addition (Fig. 6B) that correlate with the decreases in Suz12 observed in both cell lines (Fig. 6A).

The H3K27 residue can also be acetylated, which is frequently associated with transcriptional activation[33]. Increased acetylation on H3K27 near the *Hoxa1* RARE contributes to RA-induced transcriptional activation of Hoxa1 by RA[34]. Therefore, we measured H3K27ac levels near the *CRABP2* RARE1 and near the *NR2F1* P$_{RefSeq}$ region +/- RA in the WT and *CARM1 KO* cell lines. We found that in the WT cells the H3K27ac mark increased near the *CRABP2* RARE1 at 48 and 72 hrs after RA addition, but this mark did not change near the *NR2F1* P$_{RefSeq}$ region (Fig. 6C). In the *CARM1 KO* cells the levels of H3K27ac decreased by 2.53-fold ± 0.39 SE (p<0.05) and 3.1- fold ± 0.52 SE (p<0.05) at 48 and 72 hrs after RA treatment, respectively, near the *CRABP2* RARE1 (Fig. 6C). These results highlight the differential epigenetic signatures that may contribute to the RA-induced increases in *CRABP2* and *NR2F1* transcript levels in the WT cells. Overall loss of CARM1 affects Suz12 recruitment and its corresponding repressive H3K27me3 mark near the *NR2F1* P$_{RefSeq}$ region and the activating H3K27ac mark near the *CRABP2* RARE1.

DISCUSSION

Identification of a novel subset of RA-target genes that require CARM1.

Given the important role RA signaling plays in stem cell differentiation and development[1, 2], we determined the role of CARM1 in RA-induced ESC differentiation using our stable CARM1 KD and *CARM1 KO* mESC lines. We show that CARM1 is required for the RA-induction of a subset of RA-inducible genes (*CRABP2, Cyp26b1, NR2F1,* and *NR2F2*). Our results delineate at least two groups of RA-inducible target gene sets, one of which is affected by CARM1 depletion. These results suggest different mechanisms of action responsible for maximal gene induction by RA and demonstrate the importance of epigenetic regulatory proteins, such as CARM1, for these processes in mESCs.

CARM1 is required for RA-induced differentiation of mESCs into extraembryonic endoderm.

The impaired differentiation of these *CARM1 KO* mESCs along the extraembryonic endoderm lineage highlights the importance of CARM1 in RA-induction of *NR2F1* transcript levels, as NR2F1 is a transcription factor involved in specific differentiation programs[27]. RA-induction of NR2F1 has been reported to repress expression of the differentiation associated homeobox transcription factor *Cdx1* in the caudal embryo[35]. This occurs via the ability of NR2F1 to compete with RXR/RAR binding specifically at the RARE of *Cdx1*[35]. In P19 embryonal carcinoma cells, NR2F1 can also repress Oct4[36] by competing with RXR/RAR binding at the RAREoct site of *Oct4*[36]. We did not see an effect of the loss of CARM1 on Oct4 expression, and future work is needed to determine if the absence of NR2F1 expression subsequent to depletion of CARM1 affects RA-induction of *Cdx1* transcripts. CARM1 loss may

12

facilitate or block differentiation into other germ layers, but the reduced RA-induction of *Gata4*, *Gata6*, *Lamβ1*, *PDGFRα*, *Sox7*, and *Sox17* transcripts we detected in the *CARM1 KO* cells indicates that CARM1 is required for the differentiation of mESCs into extraembryonic endoderm, potentially through NR2F1's regulation of these extraembryonic endoderm genes.

CARM1 is not required for pluripotency in ES stable KD and KO cells.

Previous studies have shown that the short-term loss of CARM1 results in spontaneous differentiation of untreated mESCs[21, 22] and that CARM1 activity results in preferential contribution of cells to the inner cell mass rather than the trophectoderm[37, 38]. We have shown that ES cells without CARM1 functionally behave like ES cells and express the pluripotency transcripts of *Nanog*, *Oct4*, *Rex1*, and *Sox2*. We note that one difference between our data and those of other groups[21, 22] is that we generated stable CARM1 depletion mESC lines by shRNA and CRISPR/Cas9 methodologies, whereas other reports[21, 22] described the use of cells in which CARM1 was knocked down for three and eight days by siRNA technology[21, 22]. We used CRISPR/Cas9 as a complementary method to target CARM1 for depletion to avoid possible off-target effects from siRNA methodology[39]. After stable CARM1 loss in the mESCs, we detected no differences in the basal expression of pluripotency transcripts. It is known that CARM1 is necessary for normal development since CARM1$^{-/-}$ mice are not viable and die shortly after birth[40, 41]. However, these CARM1$^{-/-}$ mice are able to develop throughout their full term and die primarily from defects such as the improper differentiation of their myosatellite cells, adipocytes, and pulmonary epithelial cells during development[14, 40, 42, 43]. Importantly, in the *CARM1 KO* cells the transcript levels of *Rex1* (*Zfp42*) remained high even in the presence of RA, suggesting that CARM1 is

required for RA to negatively regulate the transcript levels of the stem cell marker, Rex1[44].

The complex epigenetic dynamics involved in controlling gene activation during RA-induced differentiation of CARM1 target genes.

Although the *Hoxa1*, *CRABP2*, and *NR2F1* genes studied here are all known to be increased at the mRNA level by RA treatment in WT ESCs[1, 2, 23, 24], our results show differences in their epigenetic regulation following the addition of RA. These findings support a distinction between different groups of RA-inducible genes based on how they are regulated at the epigenetic level[18]. Moreover, Gillespie and Gudas[45] showed that Suz12 was removed from the Hoxa1 and RARβ2 RAREs within 30 min. – 4 hrs after RA addition. Laursen *et al.*[18] reported that knockdown of the Suz12 protein in the PRC2 complex in mESCs further increased the transcript levels of *NR2F1* and *NR2F2* after RA treatment[18]. Here we found that upon depletion of the CARM1 protein *NR2F1/2* transcripts are induced after RA addition to a lesser extent than in the parental WT and shCtl mESC lines. The H3R26me2 modification is favored by acetylation of K27[46], and we therefore speculate that the opposing effects of CARM1 and Suz12 on the regulation of NR2F1 may reflect mutually exclusive histone modifications.

To determine if CARM1 binding is necessary for the RA-induction of CARM1 target genes, we performed ChIP-qPCR analyses in WT mESCs. We focused on the *NR2F1* and *CRABP2* loci as representative of genes that require CARM1 for RA-induction and *Hoxa1* as a gene that does not require CARM1 for RA-induction. In the WT mESCs we found that CARM1 and H3R17me2a were present in the absence of RA near the P_{RefSeq} region of *NR2F1* and near RARE1 of *CRABP2*, but contrary to our hypothesis, CARM1 and H3R17me2a levels did not increase at these regions upon RA

14

addition to the WT mESCs. We also detected CARM1 binding near the *Hoxa1* RARE in WT mESCs. CARM1 is detected near the *Hoxa1* RARE, but the RA-induction of *Hoxa1* is not dependent on CARM1 levels in WT cells. Our results show that an *increase* in CARM1 occupancy near the *NR2F1* P$_{RefSeq}$ promoter and RARE1 of *CRABP2* is not necessary for the RA-induction of *CRABP2* and *NR2F1* in WT cells, but CARM1 is required for RA to increase their transcript levels (Fig. 7 for model).

Application of newly identified CARM1 effects in other cellular contexts.

Our work in identifying RA-induced genes regulated by CARM1 in WT mESCs allows us to expand the growing list of CARM1 targets identified over the past few years[10, 17, 20, 42, 43, 47, 48]. Other substrates of CARM1 include transcription factors (Pax7 and RUNX1)[42, 47], splicing factors (CA150)[48], and transcriptional coactivators (p300/CBP, NCoa3)[10, 17, 49]. Identification of these substrates and others has implicated overexpression of CARM1 in the progression of breast cancer[12, 20] and in the differentiation of different cell types[14, 40, 42, 43]. The different functions of CARM1 targets emphasize its versatility as a PRMT and/or coactivator and establish CARM1 as important for a variety of different cellular processes, now including mESC RA-induced differentiation. From our list of genes requiring CARM1, the two exemplary genes that we focused on are *NR2F1* and *CRABP2* since some data has been published concerning their RA regulation[18, 24]. Additionally, *NR2F1* and *CRABP2* have been implicated in diseases such as cancer[50, 51], and NR2F1 is important for neurogenesis and is highly expressed in the nervous system during development[52]. Since the roles of other PRMTs have been studied in RA-induced neuronal differentiation of ESCs[4, 5], in future work it will be illuminating to determine if CARM1 plays a role in RA-induced neuronal differentiation of ESCs given its role in regulating NR2F1 in our ESC model of

15

differentiation into parietal endoderm cells.

In conclusion, our study highlights a novel role for CARM1 in RA-induced ESC differentiation and defines how CARM1 is required for the induction of key RA-inducible genes. In this study we identified novel genes regulated by CARM1 and uncovered a requirement for CARM1 in the RA-induced differentiation of ESCs into extraembryonic endoderm.

Materials and Methods

Cell culture.

J1 murine embryonic stem cell lines were plated and grown in gelatin-coated plates as described[18]. All cell counts were performed using a cell and particle counter (Z1 Particle Counter; Beckman-Coulter).

Generation of CARM1 knockdown (KD) J1 mESCs via shRNA lentiviral transduction.

HEK293T cells were co-transfected with either 20 µg pLKO.1-puro CARM1 shRNA (Sigma, cat# TRCN0000039117, "sh9117": 5'-CCGGCCACGATTTCTGTTCTTTCTACTCGAGTAGAAAGAACAGAAATCGTGGTTTTTG-3') or shscramble control vector (Sigma, cat# SHC002), 15 µg packaging plasmid pCMVΔR8.9, and 5 µg envelop plasmid pVSV-G using Lipofectamine 2000 (Invitrogen). Lentiviral particles were collected after 48 hrs and infected into J1 WT mESCs with polybrene (10 µg/mL). After 48 hrs, cells were grown in 5 µg/mL puromycin selection media for 1-2 weeks to develop antibiotic resistant colonies.

Generation of *CARM1 KO* J1 mESCs via CRISPR/Cas9 Flip 'n' Glow.

CARM1Ex4 (105bp) is inverted by cre-mediated recombination to cause loss of Carm1 function by introducing a fusion with EGFP after exon 3. The Carm1-EGFP transition codes for SSAVNYFN-F*MVSK*GEELFT (italics indicate EGFP). Expression of the EGFP fusion is controlled by the CARM1 promoter. We ligated the pBig CARM1-EGFP template DNA (5'-Pm1I, 3'-BglII) into the 5'-AscI, 3'-PacI sites of pX330 CARM1-I3F/CARM1-I4F (Cas9-WT KBL#409/408) construct. PCR-analysis was used to confirm WT, knock-in (KI), and recombined (KO) CARM1.

RA treatments and RNA isolation.

J1 mESC lines were treated with vehicle (0.1% EtOH) or 1 µM RA for 24-72 hrs, with RA replaced every 48 hrs. Total RNA was isolated using TRIzol (Invitrogen) according to the manufacturer's protocol. RNA (2 µg) was reverse-transcribed to cDNA using qScript (Quanta Biosciences). 2 µL of 1:10 diluted cDNA was used for all semi-quantitative (sq)-PCR reactions.

Semi-quantitative and quantitative RT-PCR analyses.

cDNA RT-PCR amplification for sq-PCR was performed using Taq DNA polymerase (Invitrogen) (20 µL reaction volume). Using a Bio-Rad iCycler, each cycle included: denaturation: 95°C (30s), annealing: 58–65°C (30s), and extension: 72°C (45s). PCR products were separated by electrophoresis on an ethidium bromide stained 1-2% agarose gel. ImageJ software (National Institutes of Health) was used to quantitate band densities and we normalized cDNA product to the internal reference gene *36B4*. qRT-PCR reactions (15 µL) were carried out using SYBR Green quantitative PCR master mix. Specific primer sequences for each gene are shown (Supplemental Table 2).

Protein extraction and Western Blot analysis.

We isolated protein[53] and performed western blotting (25-30 µg protein) as previously described[54] using the following primary antibodies: anti-CARM1 (Millipore, cat# 09-818, lot# 2036700, 1:1000); anti-Actin (Cell Signaling, cat# MAB1501, lot# 2275539 & 2665057, 1:80,000); anti-me-PABP1 (gift from Dr. Wei Xu, 1:1000); anti-Nanog (Cell Signaling, cat# 4903P, lot# 1, 1:1000); anti-Oct3/4 (Santa Cruz, cat# 8629, lot# K1308, 1:250), and secondary antibodies: anti-goat (Santa Cruz, cat# sc2020, lot #H1715, 1:10,000); anti-rabbit (Jackson ImmunoResearch, cat# 715-035-152, lot#

1117118 & 22884, 1:10,000); anti-mouse (Jackson ImmunoResearch, cat# 715-035-150, lot# 116722 & 123115, 1:10,000). Membranes were developed using the Western Pierce ECL Plus Substrate kit (ThermoFisher).

Chromatin Immunoprecipitation (ChIP) assays.

We cultured J1 WT and *CARM1 KO* #23 cells with or without 1 µM RA for 24-72 hrs. Cells were plated at ~0.3 x 10^6 (72 hr), ~ 0.9 x 10^6 (48 hr), and ~2.5 x 10^6 (24hr) on consecutive days to collect all time points for ChIP processing on the same day. Cells were crosslinked using a one-step (H3K27ac, H3K27me3) or two-step (CARM1, Suz12) ChIP protocol as described previously in the lab[54, 55]. Cells were sonicated and the precleared lysates (25 µg DNA) were immunoprecipitated using 0.5–2.0 µg of antibodies specific for CARM1 (Epicypher, Research Triangle Park, NC, cat# 13-0006, lot# 13281001), H3K27ac (Abcam, cat# 4729, lot# GR28147), H3K27me3 (Abcam, cat# 6002, lot# 2736613), H3R17me2a (Abcam, cat# 8284, lot# GR295369-1), Suz12 (Cell Signaling, cat# D39F6, lot# 3), or IgG (Santa Cruz, cat# sc2027, lot# L2414) (negative control). We purified DNA using the Qiagen PCR purification kit and used 3 µL for qPCR analysis. We used DNA input samples diluted 1:10 (2.5 µg) to normalize immunoprecipitated DNA. ChIP analyses were performed at least three times for each IP (n ≥ 3).

RNA-seq/Genome-wide Transcriptomics.

J1 WT, shCtl, and CARM1 KD cells were treated with or without RA as described above for 48 hrs. We extracted RNA using the Qiagen RNeasy Plus Kit. Samples were submitted to the Weill Cornell Genomics Resources Core Facility for Next-Generation Sequencing (RNA-Seq) as previously described[56]. The total number reads and the number of aligned reads are listed in Supplemental Table 3. Dr. Tuo Zhang (Weill

Cornell Genomics Core Facility) aligned the reads to the mouse mm9 reference genome using Tophat2[57] and gene expression values were measured in RPKM using cufflinks[58]. The RNA-seq data were deposited in GEO (NCBI) repository under accession number GSE115818.

We filtered our RNA-seq data for genes that were ≥ 2-fold increased with RA treatment in the shCtl cells compared to the vehicle treated shCtl cells. We set a cutoff of 0.5 RPKM in the shCtl RA treated cells, which resulted in 2,840 genes. We also considered genes whose values were ≥ 1.5-fold increased with RA in the J1 parental cells and ≥ 0.5 RPKM. RA-induction of most transcripts was higher in the shCtl cells compared to the J1 parental cells and chose 1.5 rather than 2-fold RA-induction in the parental cells as one of our parameters. This resulted in 2,356 genes induced by RA in the J1 parental and shCtl control cell lines. We next considered genes whose transcript levels were ≥ 2-fold higher in the shCtl RA treated cells and ≥ 1.5-fold higher in the J1 parental RA-treated cells compared to the CARM1 KD RA-treated cells. This resulted in 101 genes whose RA-induction requires CARM1.

Statistical analyses of data.

We used Microsoft Excel to calculate the mean values and standard errors of mean (SE). Transcript levels are normalized to *36B4* or *HPRT* and protein expression is normalized to Actin. We used one-way ANOVA followed by the Tukey post hoc test to determine statistical significance among groups (GraphPad Prism 7). Values for ChIP-qPCR are normalized to their respective input samples and represented as relative occupancy to the J1 vehicle control sample, set to 1. We used student's t-test to compare the two cell lines at each time point for ChIP-qPCR analysis.

Acknowledgements.

References:

1. Gudas L. J. (2013). Retinoids induce stem cell differentiation via epigenetic changes. Semin Cell Dev Biol. 24(10-12), 701-705.

2. Gudas L.J. & Wagner J. A. (2011). Retinoids regulate stem cell differentiation. J Cell Physiol. 226(2), 322-330.

3. Chen T. & Dent S. Y. (2014). Chromatin modifiers and remodellers: regulators of cellular differentiation. Nat Rev Genet. 15(2), 93-106.

4. Simandi Z., Czipa E., Horvath A., et al. (2015). PRMT1 and PRMT8 regulate retinoic acid-dependent neuronal differentiation with implications to neuropathology. Stem Cells. 33(3), 726-741.

5. Stein C., Nötzold R. R., Riedl S., et al. (2016). The arginine methyltransferase PRMT6 cooperates with polycomb proteins in regulating HOXA gene expression. PLoS One. 11(2), e0148892.

6. Bedford M.T. & Richard S. (2005). Arginine methylation an emerging regulator of protein function. Mol Cell. 18(3), 263-272.

7. Chen D., Ma H., Hong H., et al. (1999). Regulation of transcription by a protein methyltransferase. Science. 284(5423), 2174-2177.

8. Kuhn P., Chumanov R., Wang Y., et al. (2011). Automethylation of CARM1 allows coupling of transcription and mRNA splicing. Nucleic Acids Res. 39(7), 2717-2726.

9. Lee Y. H. & Stallcup M. R. (2011). Roles of protein arginine methylation in DNA damage signaling pathways is CARM1 a life-or-death decision point? Cell Cycle. 10(9), 1343-1344.

10. Xu W., Chen H., Du K., et al. (2001). A transcriptional switch mediated by cofactor methylation. Science. 294(5551), 2507-2511.

11. Xu W., Cho H., Kadam S., et al. (2004). A methylation-mediator complex in hormone signaling. Genes Dev. 18(2), 144-156.

12. Yang Y. & Bedford M. T. (2013). Protein arginine methyltransferases and cancer. Nat Rev Cancer. 13(1), 37-50.

13. Bedford M. T. & Clarke S. G. (2009). Protein arginine methylation in mammals: who, what, and why. Mol Cell. 33(1), 1-13.

14. Yadav N., Cheng D., Richard S., et al. (2008). CARM1 promotes adipocyte

differentiation by coactivating PPARgamma. EMBO Rep. 9(2), 193-198.

15. Millard C. J., Watson P. J., Fairall L., et al. (2013). An evolving understanding of nuclear receptor coregulator proteins. J Mol Endocrinol. 51(3), T23-36.

16. Lee E., Madar A., David G., et al. (2013). Inhibition of androgen receptor and β-catenin activity in prostate cancer. Proc Natl Acad Sci USA. 110(39), 15710-15715.

17. Wu Z., Yang M., Liu H., et al. (2012). Role of nuclear receptor coactivator 3 (Ncoa3) in pluripotency maintenance. J Biol Chem. 287(45), 38295-38304.

18. Laursen K. B., Mongan N. P., Zhuang Y., et al. (2013). Polycomb recruitment attenuates retinoic acid-induced transcription of the bivalent NR2F1 gene. Nucleic Acids Res. 41(13), 6430-6443.

19. Lee J. & Bedford M. T. (2002). PABP1 identified as an arginine methyltransferase substrate using high-density protein arrays. EMBO Rep. 3(3), 268-273.

20. Wang L., Zhao Z., Meyer M. B., et al. (2014). CARM1 Methylates Chromatin Remodeling Factor BAF155 to Enhance Tumor Progression and Metastasis. Cancer Cell. 25(1), 21-36.

21. Wu Q., Bruce A. W., Jedrusik A., et al. (2009). CARM1 is Required in Embryonic Stem Cells to Maintain Pluripotency and Resist Differentiation. Stem Cells. 27(11), 2637-2645.

22. Xu Z., Jiang J., Xu C., et al. (2013). MicroRNA-181 regulates CARM1 and histone arginine methylation to promote differentiation of human embryonic stem cells. PLoS One. 8(1), e53146.

23. Ross A. C. & Zolfaghari R. (2011). Cytochrome P450s in the Regulation of Cellular Retinoic Acid Metabolism. Annu Rev Nutr. 31, 65–87.

24. Durand B., Saunders M., Leroy P., et al. (1992). All-trans and 9-cis retinoic acid induction of CRABPII transcription is mediated by RAR-RXR heterodimers bound to DR1 and DR2 repeated motifs. Cell. 71(1), 73-85.

25. Budhu A. S. & Noy N. (2002). Direct Channeling of Retinoic Acid between Cellular Retinoic Acid-Binding Protein II and Retinoic Acid Receptor Sensitizes Mammary Carcinoma Cells to Retinoic Acid-Induced Growth Arrest. Mol Cell Biol. 22(8), 2632-2641.

26. Martinez-Ceballos E. & Gudas L. J. (2008). Hoxa1 is required for the retinoic acid-

induced differentiation of embryonic stem cells into neurons. J Neurosci Res. 86(13), 2809-2819.

27. Zhuang Y. & Gudas L. J. (2008). Overexpression of COUP-TF1 in murine embryonic stem cells reduces retinoic acid-associated growth arrest and increases extraembryonic endoderm gene expression. Differentiation. 76(7), 760-771.

28. Paca A., Séguin C. A., Clements M., et al. (2012). BMP signaling induces visceral endoderm differentiation of XEN cells and parietal endoderm. Dev Biol. 361(1), 90-102.

29. Langston A. W. & Gudas L. J. (1992). Identification of a retinoic acid responsive enhancer 3 of the murine homeobox gene Hox-1.6. Mech. Dev. 38(3), 217-227.

30. Lee J. S., Smith E., & Shilatifard A. (2010). The Language of Histone Crosstalk. Cell. 142(5), 682-685.

31. Daujat S., Bauer U. M., Shah V., et al. (2003). Crosstalk between CARM1 methylation and CBP acetylation on histone H3. Curr Biol. 12(24), 2090-2097.

32. Pasini D., Bracken A. P., Hansen J. B., et al. (2007). The polycomb group protein Suz12 is required for embryonic stem cell differentiation. Mol Cell Biol. 27(10), 3769-3779.

33. Wang Z., Zang C., Rosenfeld J. A., et al. (2008). Combinatorial patterns of histone acetylations and methylations in the human genome. Nat Genet. 40(7), 897-903.

34. Urvalek A. M. & Gudas L. J. (2014). Retinoic acid and histone deacetylases regulate epigenetic changes in embryonic stem cells. J Biol Chem. 289(28), 19519-19530.

35. Béland M. & Lohnes D. (2005). Chicken ovalbumin upstream promoter-transcription factor members repress retinoic acid-induced Cdx1 expression. J Biol Chem. 280(14), 13858-13862.

36. Ben-Shushan E., Sharir H., Pikarsky E., et al. (1995). A dynamic balance between ARP-1/COUP-TFII, EAR-3/COUP-TFI, and retinoic acid receptor:retinoid X receptor heterodimers regulates Oct-3/4 expression in embryonal carcinoma cells. Mol Cell Biol. 15(2), 1034-1048.

37. Torres-Padilla M. E., Parfitt D. E., Kouzarides T., et al. (2007). Histone arginine methylation regulates pluripotency in the early mouse embryo. Nature. 445(7124), 214-218.

38. Goolam M., Scialdone A., Graham S. J., et al. (2016). Heterogeneity in Oct4 and

Sox2 Targets Biases Cell Fate in 4-Cell Mouse Embryos. Cell. 165(1), 61-74.

39. Caffrey D. R., Zhao J., Song Z., et al. (2011). siRNA off-target effects can be reduced at concentrations that match their individual potency. PLoS One. 6(7), e21503.

40. Kim D., Lee J., Cheng D., et al. (2010). Enzymatic activity is required for the in vivo functions of CARM1. J Biol Chem. 285(2), 1147-1152.

41. Yadav N., Lee J., Kim J., et al. (2003). Specific protein methylation defects and gene expression perturbations in coactivator-associated arginine methyltransferase 1-deficient mice. Proc Natl Acad Sci USA. 100(11), 6464-6468.

42. Kawabe Y., Wang Y. X., McKinnell I. W., et al. (2012). Carm1 regulates Pax7 transcriptional activity through MLL1/2 recruitment during asymmetric satellite stem cell divisions. Cell Stem Cell. 11(3), 333-345.

43. O'Brien K. B., Alberich-Jordà M., Yadav N., et al. (2010). CARM1 is required for proper control of proliferation and differentiation of pulmonary epithelial cells. Development. 137(13), 2147–2156.

44. Hosler B. A., LaRosa G. J., Grippo J.F., et al. (1989). Expression of REX-1, a gene containing zinc finger motifs, is rapidly reduced by retinoic acid in F9 teratocarcinoma cells. Mol Cell Biol. 9(12), 5623-5629.

45. Gillespie R. F. & Gudas L. J. (2007). Retinoid regulated association of transcriptional co-regulators and the polycomb group protein SUZ12 with the retinoic acid response elements of Hoxa1, RARβ$_2$, and Cyp26A1 in F9 embryonal carcinoma cells. J Mol Bio. 372(2), 298-316.

46. Zhang Z., Nikolai B. C., Gates L. A., et al. (2017). Crosstalk between histone modifications indicates that inhibition of arginine methyltransferase CARM1 activity reverses HIV latency. Nucleic Acids Res. 45(16), 9348-9360.

47. Vu L. P., Perna F., Wang L., et al. (2013). PRMT4 blocks myeloid differentiation by assembling a methyl-RUNX1-dependent repressor complex. Cell Rep. 5(6), 1625-1638.

48. Cheng D., Côté J., Shaaban S., et al. (2007). The arginine methyltransferase CARM1 regulates the coupling of transcription and mRNA processing. Mol Cell. 25(1), 71-83.

49. Naeem H., Cheng D., Zhao Q., et al. (2007). The Activity and Stability of the Transcriptional Coactivator p/CIP/SRC-3 Are Regulated by CARM1-Dependent

Methylation. Mol Cell Biol. 27(1), 120–134.

50. Napoli J. L. (2017). Cellular retinoid binding-proteins, CRBP, CRABP, FABP5: Effects on retinoid metabolism, function and related diseases. Pharmacol Ther. 173, 19-33.

51. Boudot A., Le Dily F., & Pakdel F. (2011). Involvement of COUP-TFs in Cancer Progression. Cancers. 3(1), 700-715.

52. Pereira F. A., Tsai M. J., & Tsai S. Y. (2000). Coup-TF orphan nuclear receptors in development and differentiation. Cell Mol.Life Sci. 57(10), 1388-1398.

53. Guo H., Wang R., Zheng W., et al. (2014). Profiling Substrates of Protein Arginine N-Methyltransferase 3 with S-Adenosyl-L-methionine Analogues. ACS Chem Biol. 9(2), 476–484.

54. Gillespie R. F. & Gudas L. J. (2007). Retinoic acid receptor isotype specificity in F9 teratocarcinoma stem cells results from the differential recruitment of coregulators to retinoic response elements. J Biol Chem. 282(46), 33421-33434.

55. Kashyap V. & Gudas L. J. (2010). Epigenetic regulatory mechanisms distinguish retinoic acid-mediated transcriptional responses in stem cells and fibroblasts. J Biol Chem. 285(19), 14534-14548.

56. Tang X. H., Osei-Sarfo K., Urvalek A. M., et al. (2014). Combination of bexarotene and the retinoid CD1530 reduces murine oral-cavity carcinogenesis induced by the carcinogen 4-nitroquinoline 1-oxide. Proc Natl Acad Sci USA. 111(24), 8907-8912.

57. Kim D., Pertea G., Trapnell C., et al. (2013). TopHat2: accurate alignment of transcriptomes in the presence of insertions, deletions and gene fusions. Genome Biol. 14(4), R36.

58. Trapnell C., Williams B. A., Pertea G., et al. (2010). Transcript assembly and quantification by RNA-Seq reveals unannotated transcripts and isoform switching during cell differentiation. Nat Biotechnol. 28(5), 511-515.
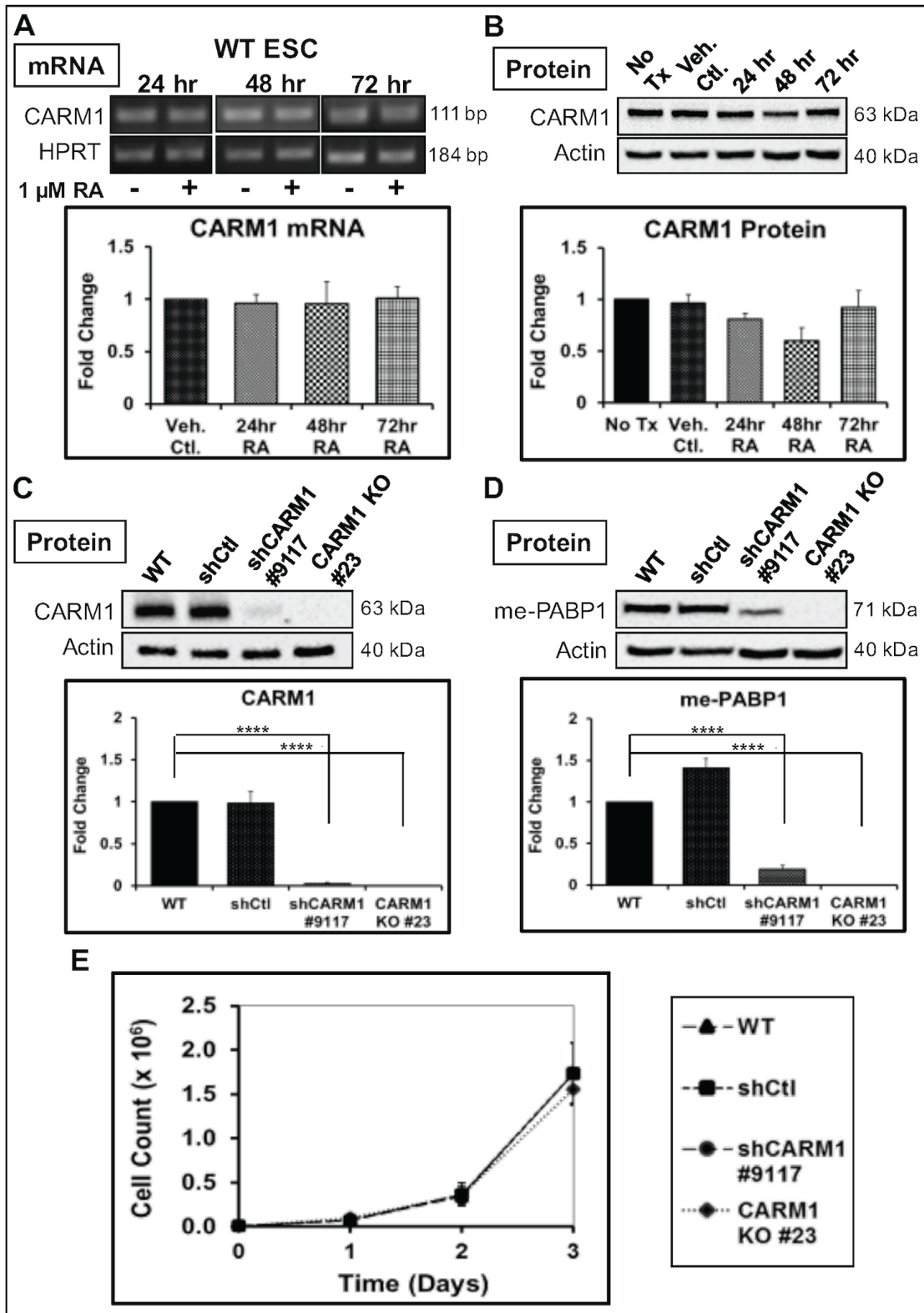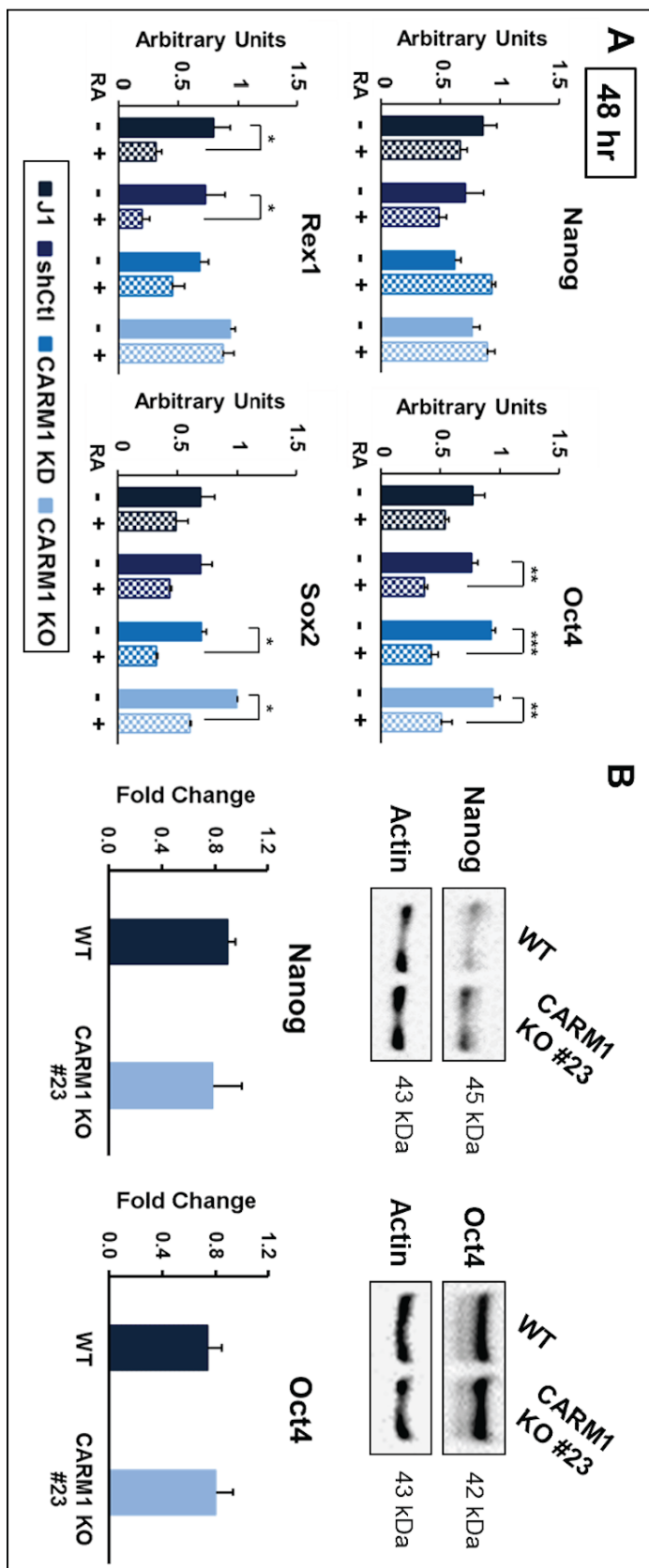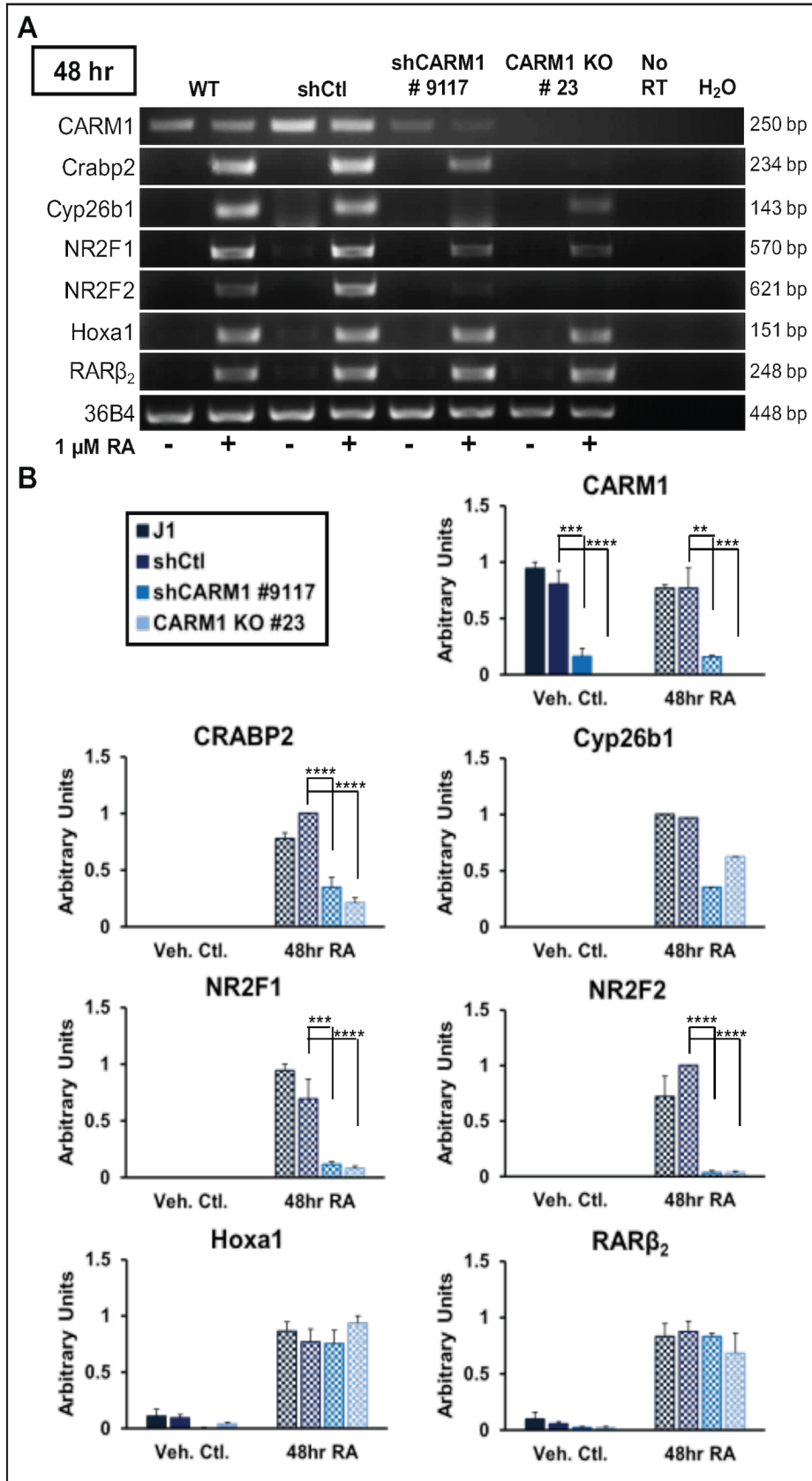
Figure 1

Figure 2

Figure 3

29
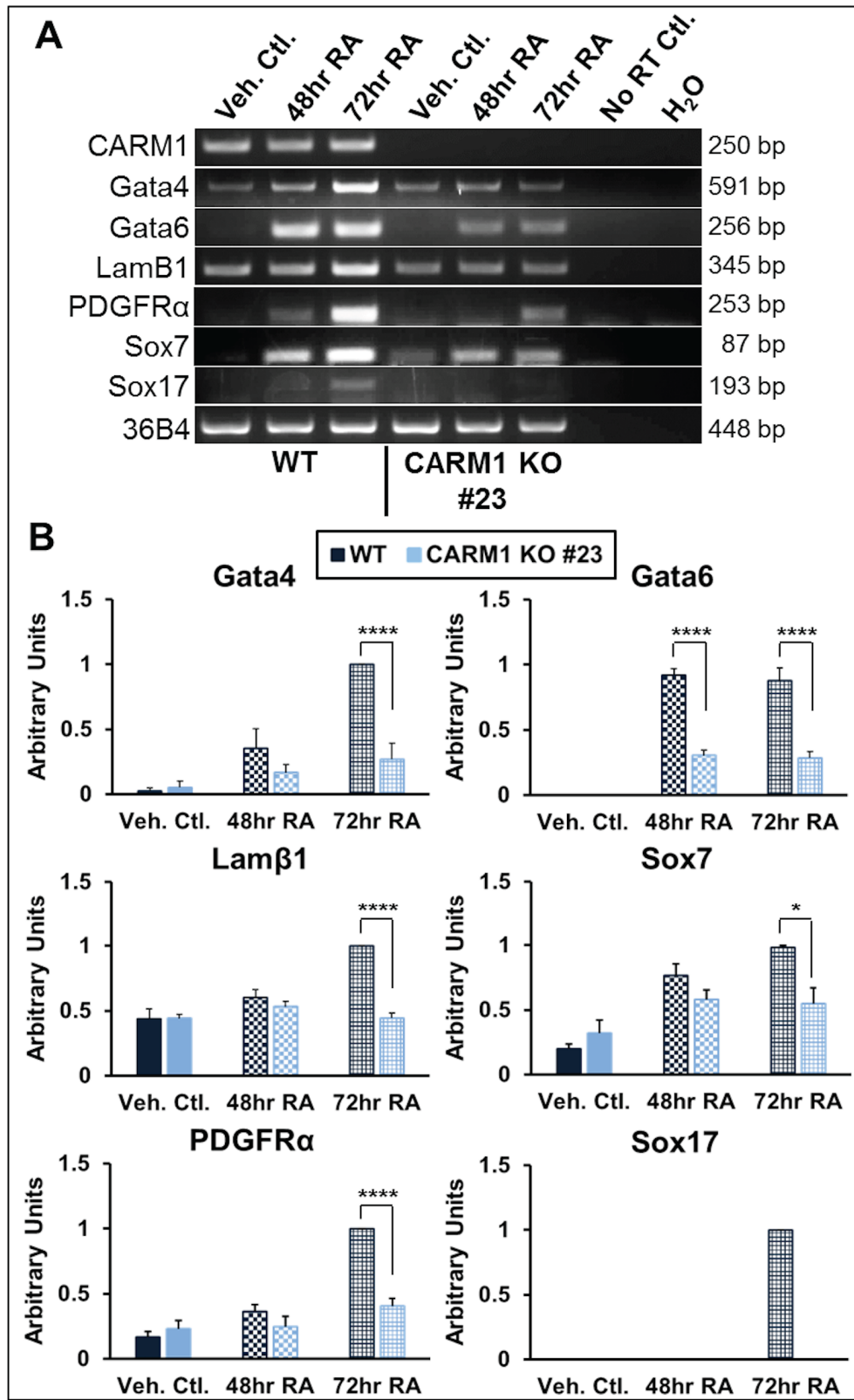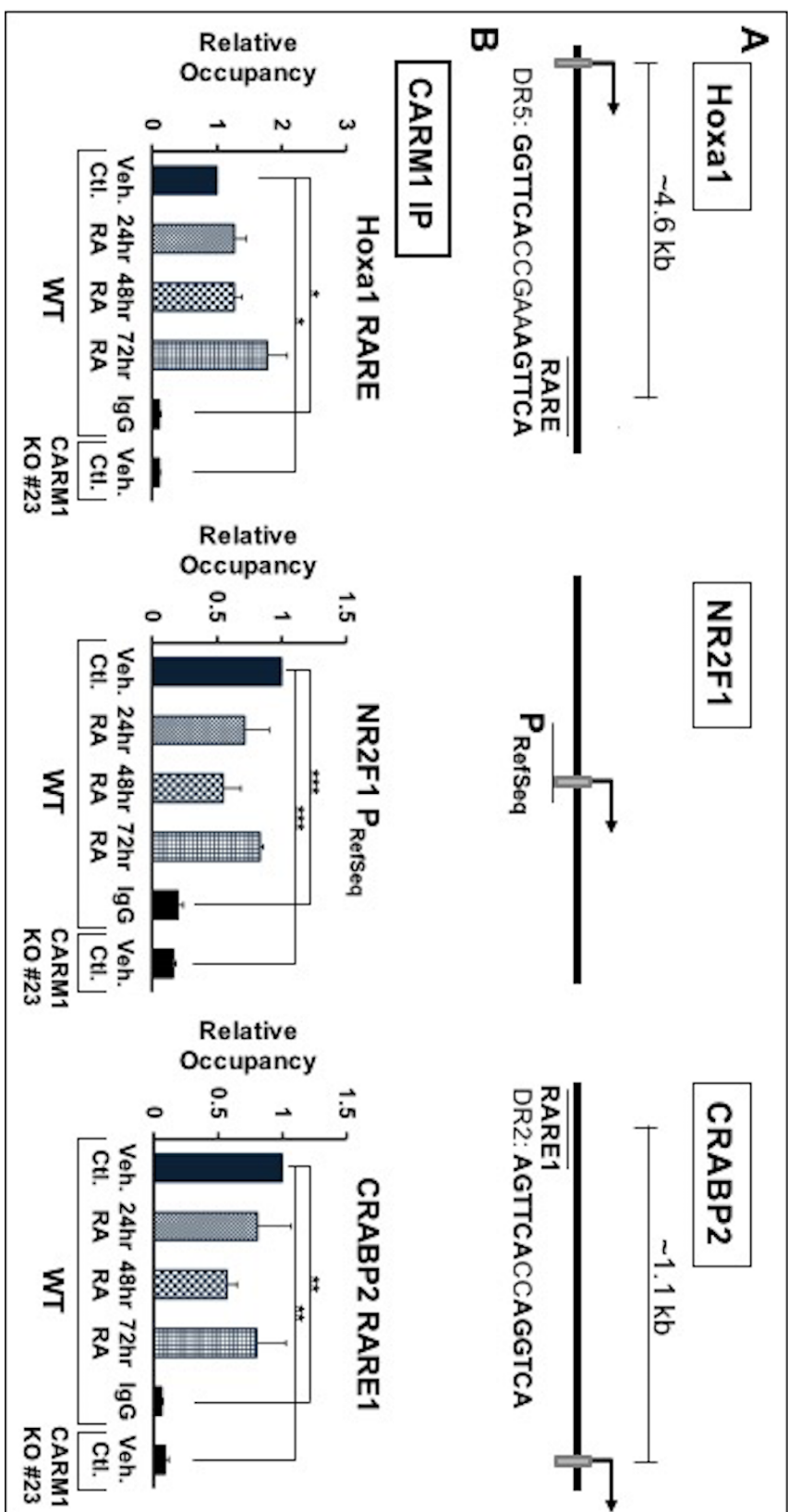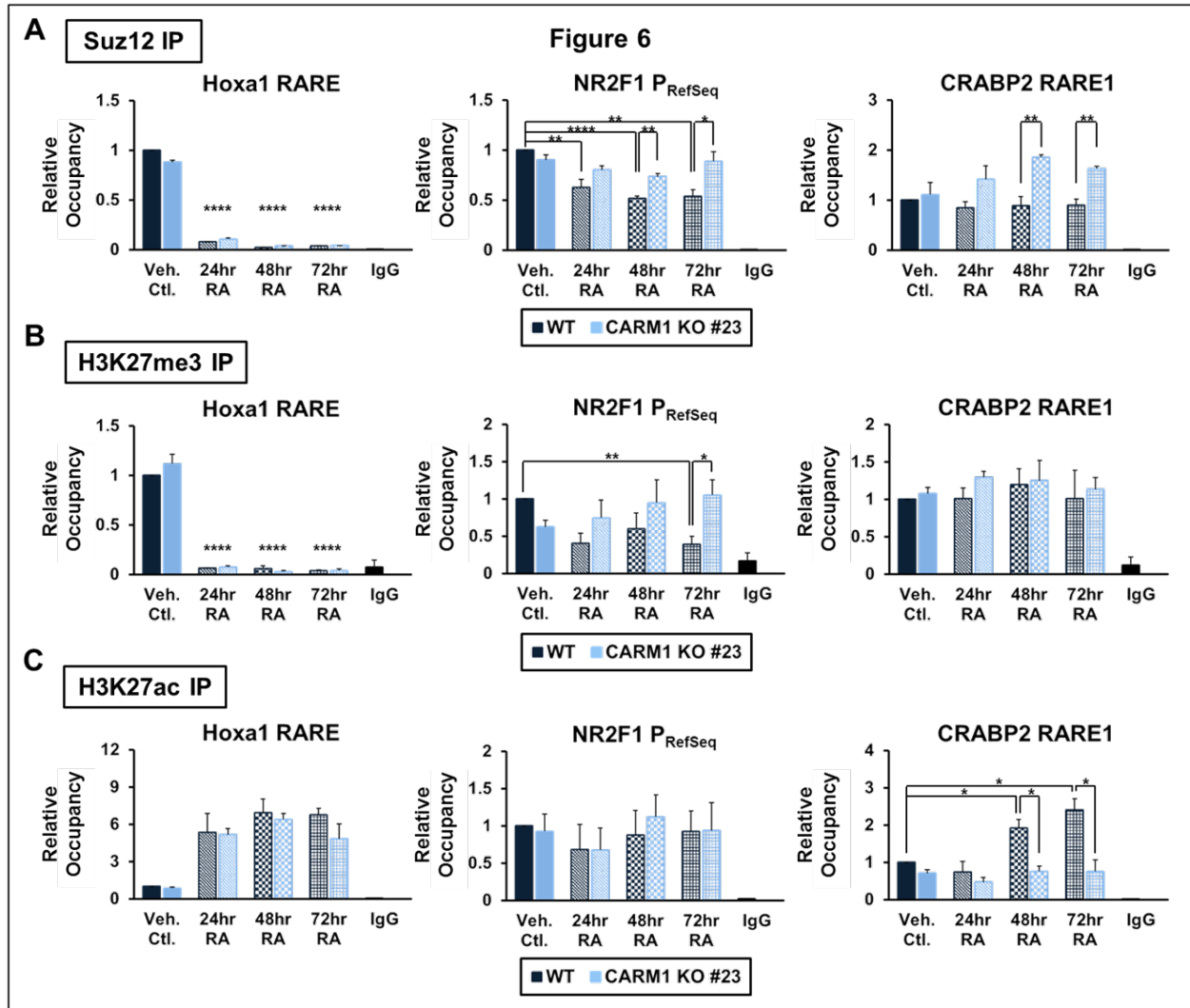
Figure 4

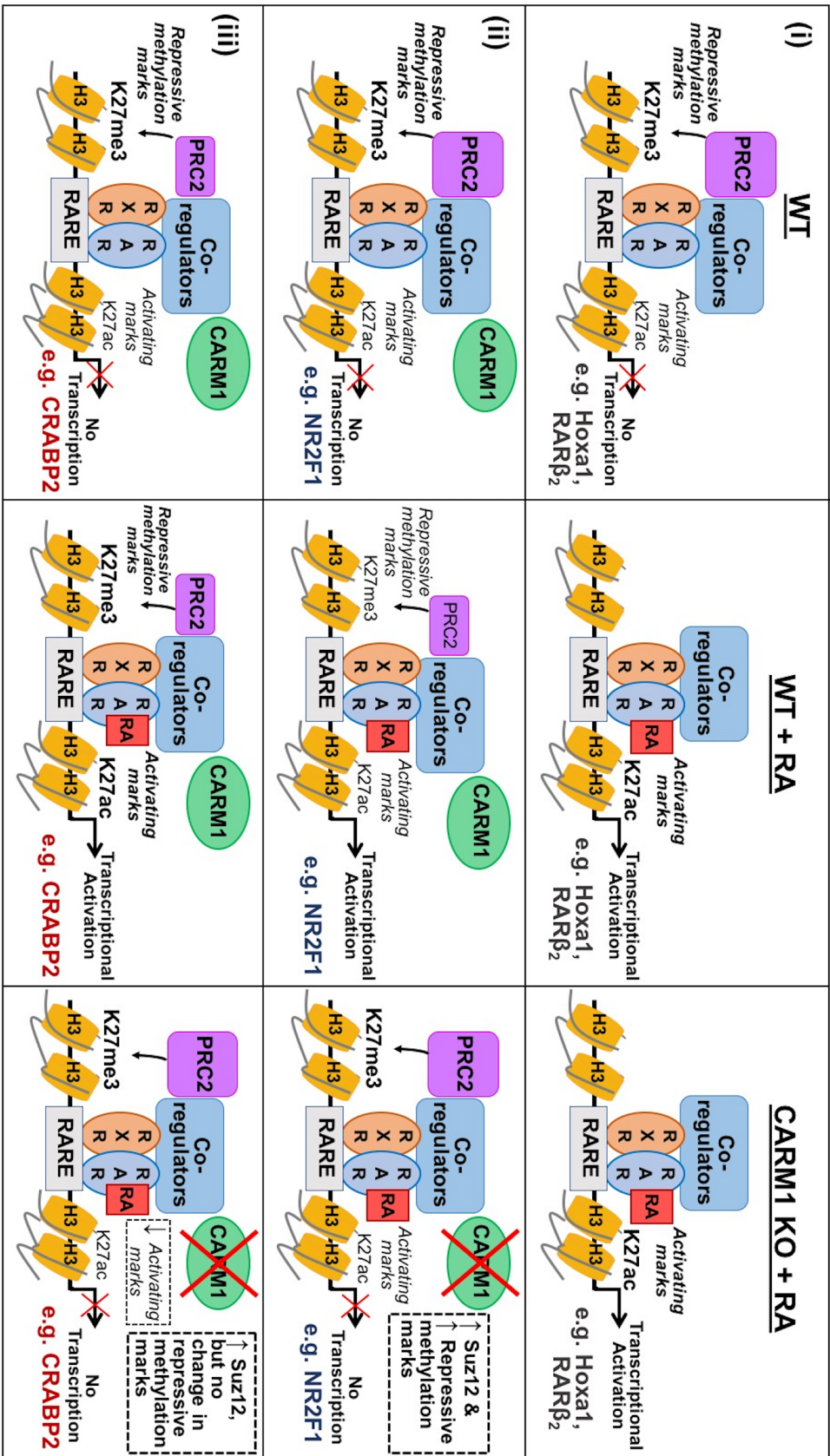**Figure 5**

Figure 6

Figure 7

FIGURE LEGENDS.

Figure 1: Generation of CARM1 KD and KO mESCs.

A) J1 WT mESCs were either treated with vehicle (Veh. Ctl.) or 1 µM RA for 24-72 hrs. *CARM1* mRNA levels were measured by semi-quantitative PCR (semi-qPCR). Images are from one experiment of three biological repeats and *HPRT* is used as the loading control to normalize *CARM1* mRNA values. **B)** J1 WT mESCs were untreated (No Tx) or treated as in A) and CARM1 protein levels were measured using western blot (WB) analysis (n=3). Actin is used as the loading control to normalize CARM1 protein values. **C)** Stable CARM1 knockdown (KD, #9117) and knockout (KO, #23) mESCs were generated as mentioned in the methods section. We used WB analysis to confirm the CARM1 KD and KO cell lines. The images are from one experiment of three biological repeats starting from the generation of lentiviral particles in HEK293T cells for the CARM1 KD cell lines. **D)** me-Pabp1 protein levels were measured by WB analysis in the CARM1 KD (#9117) and *CARM1 KO* (#23) cell lines to compare CARM1 depletion efficiency (n=3). **E)** Cell lines were plated in 12-well plates and counted 24hrs after initial plating for three consecutive days (n=3). ImageJ was used to measure mRNA band densities and Image Lab was used to measure protein band densities. Fold change is represented as the difference between each sample relative to WT Veh. Ctl, which is set to 1. Statistical significances were calculated using one-way ANOVA followed by the Tukey post hoc test (****$p<0.0001$).

Figure 2: Effects of CARM1 loss on pluripotency transcripts.

A) J1 WT, shCtl, CARM1 KD (# 9117), and *CARM1 KO* (#23) cells were plated in 6-well plates and treated with 1 µM RA for 48 hrs following 24 hrs after initial plating for

each biological repeat (n=3). mRNA levels were measured by qRT-PCR and normalized to *36B4* control mRNA levels using the delta CT method. To determine relative mRNA levels, we compared values to the highest signal, which was set to 1. **B)** J1 WT and CARM1 KO (#23) cells were plated in 6mm plates and harvested for protein isolation. Nanog and Oct4 protein levels were measured using western blot (WB) analysis. Images are from one experiment of three biological repeats. Actin is used as the loading control and Image Lab was used to measure protein band densities to generate the bar graphs. Statistical differences were calculated using one-way ANOVA followed by the Tukey post hoc test (*$p<0.05$, **$p<0.01$, ***$p<0.001$).

Figure 3: CARM1 is required for induction of a subset of RA-regulated genes.

A) J1 WT, shCtl, CARM1 KD (# 9117), and *CARM1 KO* (#23) cells were plated in 6-well plates and treated with RA for 48 hrs following 24 hrs after initial plating for each biological repeat (n=3). mRNA levels were measured by semi-quantitative PCR (semi-qPCR) and *36B4* is used as the loading control. **B)** ImageJ was used to measure the semi-qPCR band densities shown in A) to generate the bar graphs. Band densities for each gene were normalized to *36B4*. To determine relative mRNA expression, the most intense band was set to 1 (n=3, except Cyp26b1 is n=1). Statistical differences were calculated using one-way ANOVA followed by the Tukey post hoc test (**$p<0.01$, ***$p<0.001$, ****$p<0.0001$). These data were then replicated by using genome-wide RNA transcriptomic profiling (Supplemental Table 1).

Figure 4: CARM1 is required for RA-induced extraembryonic endoderm differentiation.

A) J1 WT and *CARM1 KO* (#23) cells were plated in 6-well plates and treated with RA for 48 and 72 hrs following 24 hrs after initial plating for each biological repeat (n≥3). Images are from one experiment. mRNA levels were measured by semi-quantitative PCR (semi-qPCR) and *36B4* is used as the loading control. **B)** ImageJ was used to measure the semi-qPCR band densities for each repeat to generate the bar graphs. Band densities for each gene were normalized to *36B4*. To determine relative mRNA levels, we compared values to the most intense band, which was set to 1. For Sox17, a band was only detected in the J1 parental cells at 72 hrs after RA treatment, as is seen in the gel image; therefore, significant changes could not be calculated. Statistical differences were calculated using one-way ANOVA followed by the Tukey post hoc test (****$p < 0.0001$).

Figure 5: CARM1 is present at RA responsive regions of RA-inducible target genes.

A) A representative scheme showing the regions used for chromatin immunoprecipitation (ChIP) relative to each transcriptional start site (TSS) for each gene. The bent arrows indicate the TSS. P_{RefSeq} is a putative TSS previously identified and characterized in our lab. **B)** We plated J1 WT cells in 150mm plates and 24 hrs after initial plating for each biological repeat we added 1 μM RA for 24, 48, and 72 hrs. The vehicle control (Veh. Ctl.) plates were plated at the same time as the 48hr RA plates. 25μg of ChIP lysate was used with 5μL of CARM1 antibody for the immunoprecipitation (IP). qPCR was used to measure CARM1 occupancy at each gene

region shown. IPs for IgG and *CARM1 KO* Veh. Ctl. were used as negative controls.

Graphs represent the average of three biological repeats. To determine relative

occupancy, the J1 WT Veh. Ctl. samples were set to 1 for each IP. The percent input

values set to 1 for each J1 WT Veh. Ctl. are 0.03 (Hoxa1), 004 (NR2F1), and 0.03

(CRABP2). Statistical differences were calculated using one-way ANOVA followed by

the Tukey post hoc test (*p<0.005, (**p<0.01, ***p<0.001).

**Figure 6: CARM1 depletion affects the chromatin signatures on CRABP2 and
NR2F1.**

   A) J1 WT and *CARM1 KO* (# 23) cells were plated and treated as in Fig. 5B.

25µg of ChIP lysate were used with 5µL of Suz12 antibody for the immuniprecipitation

(IP). qPCR was used to measure Suz12 occupancy at each gene region shown. The IP

for IgG is used as a negative control and the J1 WT Veh. Ctl. samples were set to 1 for

each IP to determine relative occupancy. The percent input values set to 1 for each J1

WT Veh. Ctl. are 0.70 (Hoxa1), 5.97 (NR2F1), and 0.37 (CRABP2). **B)** Cells were

plated as in A) and 2µL of the H3K27me3 antibody were used. The percent input values

set to 1 for each J1 WT Veh. Ctl. are 1.44 (Hoxa1), 0.28 (NR2F1), and 0.14 (CRABP2).

C) Cells were plated as in A) and 0.5µL of the H3K27ac antibody were used. The

percent input values set to 1 for each J1 WT Veh. Ctl. are 0.48 (Hoxa1), 0.31 (NR2F1),

and 0.43 (CRABP2). All graphs represent the average of at least three biological

repeats. We used Student's t-test to determine statistical differences at each time point

after RA treatment between the two cell lines for NR2F1 P_{RefSeq} and CRABP2 RARE1

(*p<0.05, **p<0.01, ****p<0.0001). For the Hoxa1 RARE, statistical differences were

calculated using one-way ANOVA followed by the Tukey post hoc test to compare the

J1 and KO Veh. Ctl. to J1 and KO 24-72 hrs RA samples (****p<0.0001).

Figure 7: Representative model depicting the differences between RA-inducible genes that require CARM1 (ii, iii) and those that do not (i).

In the absence of RA, CARM1 is present and both these gene sets are associated with co-repressors and repressive histone marks, such as H3K27me3. For those genes not affected upon CARM1 depletion (*e.g.* Hoxa1), Suz12 (representative of the PRC2 complex) and H3K27me3 are rapidly removed after RA addition and are no longer present at the RARE. Co-activators are then recruited to initiate transcription, along with an increase in activating histone marks (*e.g.* H3K27ac) independent of CARM1's occupancy (i). Thus, CARM1 is bound at the Hoxa1 RARE +/- RA but does not influence RA-associated transcriptional activation, so CARM1 is not shown. For genes <u>requiring</u> CARM1 for their RA-induced transcriptional activation (*i.e.* NR2F1, CRABP2), Suz12 (representative of PRC2) and the H3K27me3 mark gradually decrease (NR2F1) or do not change (CRABP2) and are not completely removed with the addition of RA in WT cells. For NR2F1, lack of CARM1 prevents the decrease in Suz12 (representative of PRC2) and the H3K27me3 mark upon RA addition (ii). Lack of CARM1 also increases Suz12 level (representative of PRC2) at the RARE1 of CRABP2, but does not affect the H3K27me3 level. There is also an increase in the H3K27ac level at CRABP2 after RA addition in WT cells, and the absence of CARM1 blocks this increase in H3K27ac (iii). There are no changes in the H3K27ac level at NR2F1 upon RA addition. CARM1 facilitates this differential modulation of epigenetic regulators upon RA treatment to allow RA-induced transcriptional activation of CRABP2 and NR2F1.